

## Space Robots Formation Control for Large Solar Sail Deployment

Mahshid Soleymani<sup>1</sup>, Maryam Kiani<sup>2</sup>

Department of Aerospace Engineering, Sharif University of Technology, Azadi Street, Tehran, Iran.

### Abstract

Solar sails use sunlight to propel a vehicle through space by reflecting solar photons off a mirror-like surface made of light reflective material. To be able to work as an interplanetary cargo-ship, the solar sail area should be large enough to receive required acceleration from the sunlight. However, mechanical deploying mechanisms are not reliable to deploy such a large solar sail. This paper presents formation control of space robots for on-orbit assembly of large solar sails. Contrary to previous works, the dynamic equations of space robots in the formation are derived by considering relative motion of the space robots with respect to the sail hub orbiting the Earth. The uncertainties including external disturbances, unmolded dynamics, and parameter uncertainties, are considered as a single time-varying term in the dynamic model. Then, an adaptive sliding mode controller combined with a second-order observer is expanded to control the on-orbit formation of space robots as well as resisting the disturbances. Finally, the efficacy of the proposed approach is demonstrated by a numerical simulation.

**Keywords:** *Solar Sail Assembly-Adaptive Sliding Mode Control-Formation Control*

### 1. Introduction

Solar sails are large, flexible, reflective surfaces that utilize the solar radiation pressure to propel in space in a similar way that kites employ the wind to lift themselves up. They are accelerated by the momentum gained from the solar photons when they hit and reflect off the sail membrane [1]. Since the solar sails use the solar energy, there is no need to supply propellant. Thus, they provide affordable propulsion, longer mission lifetimes, larger payload mass, access to unreachable orbits such as non-Keplerian and high solar latitude orbits, and high speeds in comparison with conventional propulsion systems [2]. Launched in 2010, Interplanetary Kite-craft Accelerated by Radiation of the Sun (IKAROS), made by the Japanese Aerospace Exploration Agency (JAXA), was the first demonstration of a spacecraft was being controlled by solar sails [3].

To be capable of carrying larger payloads and working as an interplanetary cargo-ship, sail's area should be increased to receive more acceleration from the sunlight [4]. For instance, to carry a payload on the order of a few tons, a sail with an area of 1 km<sup>2</sup> is required [5]. But, for these ambitious flagship-class

missions, there are some key technology challenges as follows [6]:

- Deployment of very large sail membranes
- Reducing areal density to the orders of 2.5-25 g/m<sup>2</sup>
- Degradation of sail material due to the thermal effects and ultraviolet radiation
- Attitude control of deployed solar sail
- Sail packing in a very efficient way

This paper focuses on the first issue, which is to provide an efficient solution for deployment of the sail. Generally, a mechanical mechanism must be designed in order to deploy the solar sail automatically. However, most of the mechanisms, such as the spinning expansion devices [3] and deployable booms [7], are not reliable when the sail-craft size is in the orders of several kilometers. An efficient approach that is not affected by the system size is employing the on-orbit servicing robots to pull the sail to the desired position. Moreover, the space robots can be used for other missions including assembly of the next solar sail after finishing their mission [4]. Bo and Gao [8] presented a sliding mode control approach for a formation consisting of two space robots in which a radial basis function-based neural network is employed to adjust the parameters of the control law. Queiroz et al. [9] developed a nonlinear adaptive controller to control the relative position of two spacecraft in a formation flying that overcomes the model uncertainties and external disturbances. Hu et al. [4] studied the on-orbit assembly of a 1 square kilometer solar sail employing a space robot formation. They proposed an adaptive sliding mode controller combined with a disturbance observer to control the formation of space robots. However, to simplify the dynamics and control problem, the formation of space robots has been considered as a formation of ground robots. Therefore, the formation dynamic model is a set of four scalar linear equations corresponding to the motion of four robots.

This paper develops the dynamics and control problem of Ref. [4] for on-orbit formation of space robots that has been employed to deploy the large solar sail. Contrary to Ref. [4], the full nonlinear dynamics describing the relative motion of space robots in the formation flying is considered in this paper. The orbital dynamics of the solar sail is taken into account and the motion of space robots on the solar sail is modeled as relative motion with respect to the solar sail. Thus, the dynamic model of the space robot formation will be derived as vectorial nonlinear equations. Then, the adaptive sliding mode controller combined with the

1. Ph. D. Student in Space Engineering

2. Assistant Professor, 02166164628, [kiani@sharif.edu](mailto:kiani@sharif.edu)  
(corresponding author)

disturbance observer is expanded for the obtained model of the nonlinear multi input-multi output system.

## 2. The Dynamic Model of Space Robot Formation Flying

### 2.1. Sequence of on-orbit assembly of the solar sail

The solar sail consists of a hub that contains the wrapped sail before extension, four booms as the supporting structure, and four wings in four quadrants as shown in Fig. 1 [4].

Each of the space robots has three manipulators that by employing two of them it could move on the boom while holds the sail by the third one. During the on-orbit deployment of the sail, the first and second moments of mass of the sail as well as the solar pressure and gravitational torques will change dramatically due to the large size of the sail. Thus, in order to keep the solar sail attitude stable, the sequence of on-orbit assembly is considered as shown in Fig. 2 [4]. The wings in the first and second quadrants are deployed at first and then, the other wings in the third and fourth quadrants will be expanded.

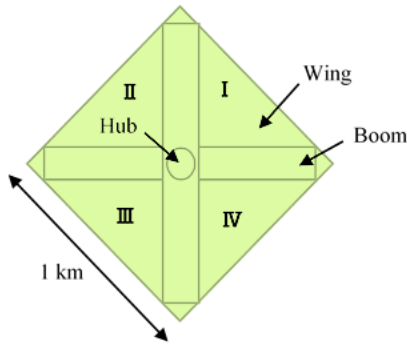


Fig. 1: The non-spinning solar sail

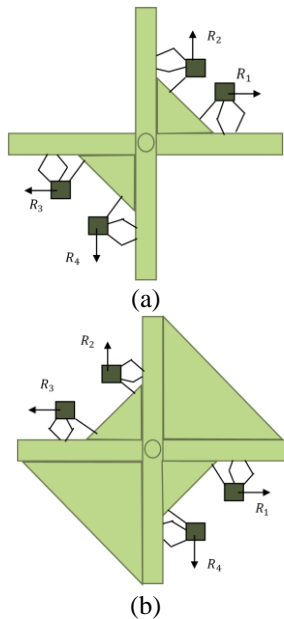


Fig. 2: The sequence of on-orbit deployment of the solar sail. (a) expanding the wing in quadrants I & III. (b) expanding the wing in quadrants II & IV.

### 2.2. Dynamic modeling

In this subsection, a nonlinear dynamic model will be derived for the space robot formation. The leader-follower approach is considered for the formation. Firstly, the equations are developed for the relative motion of the fourth robot with respect to the on-orbit solar sail and then, the relations are generalized for each of the space robots.  $R_4$  is chosen as the leader and  $R_3$  is its direct follower. Thus, the relative trajectory of  $R_4$  with respect to the solar sail is the desired trajectory, and  $R_3$  follows the actual trajectory of  $R_4$ . As the same way,  $R_2$  and  $R_1$  track the actual paths of  $R_3$  and  $R_2$ , respectively. Moreover, it is assumed that the solar sail is in a circular orbit around the Earth with a constant angular velocity  $\omega$ . The schematic representation of the relative motion of the fourth space robot with respect to the solar sail is shown in Fig. 3.

According to the Fig. 3, the following assumptions are made:

1. The inertial coordinate system  $XYZ$  is attached to the center of the earth.
2.  $\vec{R}(t) \in \mathbb{R}^3$  is the position vector from the centre of the inertial frame to the centre of the solar sail.
3. The coordinate frame  $x_s y_s z_s$  is attached to the solar sail hub so that the  $x_s$  axis in the opposite direction of tangential velocity, the  $y_s$  axis along the  $\vec{R}$  vector, and the  $z_s$  axis perpendicular to  $x_s$  and  $y_s$  establish a right handed coordinate system.
4.  $\vec{\rho}(t) \in \mathbb{R}^3$  is the relative position vector from the origin of the solar sail coordinate system to the space robot  $R_4$ .

The nonlinear dynamic equations of the solar sail and space robot  $R_4$  with respect to the inertial frame  $XYZ$  are respectively written as follows:

$$m_s \ddot{\vec{R}} + m_s (M + m_s) G \left( \frac{\vec{R}}{\|\vec{R}\|^3} \right) = \vec{u}_s + \vec{F}_s^d \quad (1)$$

$$\begin{aligned} & m_{R4} (\ddot{\vec{R}} + \ddot{\vec{\rho}}) \\ & + m_{R4} (M + m_{R4}) G \left( \frac{(\vec{R} + \vec{\rho})}{\|\vec{R} + \vec{\rho}\|^3} \right) \\ & = \vec{F}_{R4}^c + \vec{F}_{R4}^d \end{aligned} \quad (2)$$

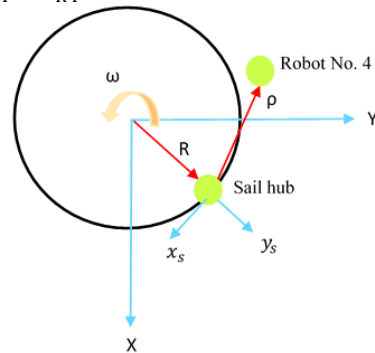


Fig. 3: schematic representation of the relative motion of the fourth space robot with respect to the solar sail from the top view

Where  $m_s$  and  $m_{R4}$  are masses,  $\vec{F}_{ds}, \vec{F}_{dR4} \in \mathbb{R}^3$  are disturbing force vectors, and  $\vec{u}_s(t), \vec{u}_{R4}(t) \in \mathbb{R}^3$  are controlling force vectors for the solar sail and space robot  $R_4$ , respectively. Also,  $M$  and  $G$  are the Earth's

mass and the universal gravity constant, respectively. Due to the fact that  $M \gg m_s, m_{R_4}$ , the Eqs. (1) and (2) are simplified as follows:

$$m_s \ddot{\vec{R}} + m_s \mu \left( \frac{\vec{R}}{\|\vec{R}\|^3} \right) = \vec{u}_s + \vec{F}_s^d \quad (3)$$

$$m_{R_4} (\ddot{\vec{R}} + \ddot{\vec{\rho}}) + m_{R_4} \mu \left( \frac{(\vec{R} + \vec{\rho})}{\|\vec{R} + \vec{\rho}\|^3} \right) = \vec{F}_{R_4}^c + \vec{F}_{R_4}^d \quad (4)$$

Where  $\mu = 398600 \text{ km}^3/\text{s}^2$  is the standard gravitational parameter. After applying some algebraic simplifications on Eqs. (3) and (4), the describing dynamic equation of the space robot  $R_4$  with respect to the solar sail expressed in the  $XYZ$  coordinate system is written as follows:

$$m_{R_4} \ddot{\vec{\rho}} + m_{R_4} \mu \left( \frac{\vec{R} + \vec{\rho}}{\|\vec{R} + \vec{\rho}\|^3} - \frac{\vec{R}}{\|\vec{R}\|^3} \right) = \vec{F}_{R_4}^c + \frac{m_{R_4}}{m_s} \vec{u}_s + \vec{F}_{R_4}^d - \frac{m_{R_4}}{m_s} \vec{F}_s^d \quad (5)$$

In order to express the Eq. (5) in the coordinate  $x_s y_s z_s$  system, first it should be noted that the relative position vector  $\vec{\rho}(t)$  is written as follows in the  $x_s y_s z_s$  coordinate system:

$$\vec{\rho} = x \hat{i}_s + y \hat{j}_s + z \hat{k}_s \quad (6)$$

Also, the constant angular velocity vector  $\omega$  equals  $\omega \hat{k}_s$ . Thus, the relative acceleration  $\ddot{\vec{\rho}}(t)$  is written in the following form:

$$\ddot{\vec{\rho}} = (\ddot{x} - 2\omega \dot{y} - \omega^2 x) \hat{i}_s + (\ddot{y} + 2\omega \dot{x} - \omega^2 y) \hat{j}_s + \ddot{z} \hat{k}_s \quad (7)$$

Moreover, the vector  $\vec{R} = \|\vec{R}\| \hat{j}_s$  is constant in the moving coordinate system  $x_s y_s z_s$ . By substituting the right hand side of Eq. (7) into the Eq. (5), the nonlinear dynamic equation of the space robot  $R_4$  with respect to the solar sail is:

$$m_{R_4} \ddot{\vec{q}} + C(\omega) \dot{\vec{q}} + N(\vec{q}, \omega, \vec{R}, \vec{u}_s) = \vec{F}_{R_4}^c + \vec{F}_{R_4}^d \quad (8)$$

Where the relative position vector  $\vec{q}(t) \in \mathbb{R}^3$  is equal to:

$$\vec{q}(t) = [x(t) \quad y(t) \quad z(t)]^T \quad (9)$$

The Coriolis matrix  $C(\omega) \in \mathbb{R}^{3 \times 3}$  is as follows:

$$C(\omega) = 2m_{R_4} \omega \begin{bmatrix} 0 & -1 & 0 \\ 1 & 0 & 0 \\ 0 & 0 & 0 \end{bmatrix} \quad (10)$$

$N(\cdot) \in \mathbb{R}^3$  is a nonlinear expression that is defined in the following form:

$$N(\vec{q}, \omega, \vec{R}, \vec{u}_s) = \begin{bmatrix} m_{R_4} \mu \frac{x}{\|\vec{R} + \vec{q}\|^3} - m_{R_4} \omega^2 x + \frac{m_{R_4}}{m_s} u_{sx} \\ m_{R_4} \mu \left( \frac{y + \|\vec{R}\|}{\|\vec{R} + \vec{q}\|^3} - \frac{1}{\|\vec{R}\|^2} \right) - m_{R_4} \omega^2 y + \frac{m_{R_4}}{m_s} u_{sy} \\ m_{R_4} \mu \frac{z}{\|\vec{R} + \vec{q}\|^3} + \frac{m_{R_4}}{m_s} u_{sz} \end{bmatrix} \quad (11)$$

Also,  $\vec{F}_d \in \mathbb{R}^3$  in Eq. (8) is the disturbance force vector that is defined as  $\vec{F}_{dR_4} = -\mu_{R_4} \vec{q}_{R_4}$ .

So far, the nonlinear dynamic equation of  $R_4$  has been achieved. The equation of motion of the space robot formation is obtained in the following form:

$$m_n \ddot{\vec{q}} + C(\omega) \dot{\vec{q}} + N(\vec{q}, \omega, \vec{R}, \vec{u}_s) = \vec{F}_n^c + \vec{F}_n^d \quad (12)$$

$n = 1, 2, 3, 4$

### 3. Controller Design

#### 3.1. Control Objective

Knowing the desired path  $\vec{q}_d(t) \in \mathbb{R}^3$  for the leader space robot  $R_4$  with respect to the solar sail, the control objective is described as follows:

$$\lim_{t \rightarrow \infty} \vec{e}_n = 0 \quad (13)$$

Where,

$$\vec{e}_n(t) = \vec{q}_n^d(t) - \vec{q}_n(t) \quad n = 1, 2, 3, 4 \quad (14)$$

The desired acceleration of robot  $R_4$  for  $t < T$  is chosen to be:

$$\ddot{\vec{q}}_{R_4}^d = [A \sin(2\pi t/T) \quad A \cos(2\pi t/T) \quad 0]^T \quad (15)$$

The desired acceleration is considered to be zero anywhere else. In Eq. (15),  $A$  and  $T$  are equal to  $1.8 \times 10^{-3}$  and 1500, respectively.

#### 3.2. Adaptive sliding mode control formulation

In this subsection, the proposed controller of Ref. [4] will be modified to control the on-orbit formation of space robots. The system dynamics (Eq. (12)) is rewritten assuming there is no control over the solar sail, i. e.  $\vec{u}_s = 0$ , as follows:

$$m_n \ddot{x} - 2m_n \omega \dot{y} + m_n \mu \frac{x}{\|\vec{R} + \vec{r}\|^3} - m_n \omega^2 x = F_{nx}^c + F_{nx}^d \quad (16)$$

$$m_n \ddot{y} + 2m_n \omega \dot{x} + m_n \mu \left( \frac{y + \|\vec{R}\|}{\|\vec{R} + \vec{r}\|^3} - \frac{1}{\|\vec{R}\|^2} \right) - m_n \omega^2 y = F_{ny}^c + F_{ny}^d \quad (17)$$

$$m_n \ddot{z} + m_n \mu \frac{z}{\|\vec{R} + \vec{r}\|^3} = F_{nz}^c + F_{nz}^d \quad (18)$$

As it can be seen from the above relations, the control force must be applied in any direction. It is clear from the Eqs. (16)-(18) that we are dealing with a multi-input-multi-output system. Since, there is a control in each direction, a sliding surface must be defined for each input. Therefore, there is a controller for each space robot that should apply the control law in each direction. The sliding surfaces are chosen as follows:

$$\vec{S}_n = [\dot{e}_{nx} + \lambda e_{nx} \quad \dot{e}_{ny} + \lambda e_{ny} \quad \dot{e}_{nz} + \lambda e_{nz}]^T \quad (19)$$

Where  $\lambda$  is a positive constant. The control law in each direction is written in the following form:

$$\vec{u}_n = \begin{bmatrix} -K_D S_{nx} - \lambda \dot{e}_{nx} - (\varepsilon_{0x} + \hat{\varepsilon}_x) \text{sign}(S_x) \\ -K_D S_{ny} - \lambda \dot{e}_{ny} - (\varepsilon_{0y} + \hat{\varepsilon}_y) \text{sign}(S_y) \\ -K_D S_{nz} - \lambda \dot{e}_{nz} - (\varepsilon_{0z} + \hat{\varepsilon}_z) \text{sign}(S_z) \end{bmatrix} \quad (20)$$

In which,  $K_D > 0$ , and  $\hat{\varepsilon}$  is updated by the following differential equations [4]:

$$\dot{\hat{\epsilon}}_n = \begin{bmatrix} \frac{1}{\kappa}(-\tau\hat{\epsilon}_{nx} + |S_{nx}|) \\ \frac{1}{\kappa}(-\tau\hat{\epsilon}_{ny} + |S_{ny}|) \\ \frac{1}{\kappa}(-\tau\hat{\epsilon}_{nz} + |S_{nz}|) \end{bmatrix} \quad (21)$$

In which,  $\kappa > 0$  is the sensitivity coefficient of  $\hat{\epsilon}$ . The smaller the  $\kappa$  is, the more sensitive the  $\hat{\epsilon}$  is to  $|S|$ . Also,  $\tau > 0$  is a small constant so that the expression  $-\tau\hat{\epsilon}$  causes  $\hat{\epsilon}$  remain a small constant when  $|S|$  is in the neighborhood of zero. Moreover, In Eq. (20),  $\epsilon_0 > 0$  is the constant part of the adaptive gain ( $\epsilon_0 + \hat{\epsilon}$ ) as well as sets the minimum uncertainty tolerance capability for the controller.

To avoid chattering,  $sign(S)$  can be replaced with the hyperbolic tangent function [4], which results in the following relationships.

$$\vec{u}_n = \begin{bmatrix} -K_D S_{nx} - \lambda \dot{\epsilon}_{nx} - (\epsilon_{0x} + \hat{\epsilon}_x) \tanh(\eta S_x) \\ -K_D S_{ny} - \lambda \dot{\epsilon}_{ny} - (\epsilon_{0y} + \hat{\epsilon}_y) \tanh(\eta S_y) \\ -K_D S_{nz} - \lambda \dot{\epsilon}_{nz} - (\epsilon_{0z} + \hat{\epsilon}_z) \tanh(\eta S_z) \end{bmatrix} \quad (22)$$

Where the scalar  $\eta$  determines the similarity between  $\tanh(\eta S)$  and  $sign(S)$ .

Eventually, the actual control forces are computed by the following relations:

$$\vec{F}_n^c = \begin{cases} m_n(\ddot{q}_n^d - \vec{u}_n) + C(\omega)\dot{q}_n + N(\vec{q}, \omega, \vec{R}), & n = N \\ \vec{F}_{n+1}^c - \vec{u}_n, & n = N - 1, \dots, 1 \end{cases} \quad (23)$$

### 3.3. Disturbance observer

As it can be seen from the Eq. (22), measuring the translational velocity of space robots is required. However, obtaining the velocity information of a maneuvering space robot is difficult and even measurement noise will be added to the system. Therefore, to improve the controller performance, the second-order observer with finite time convergence [4], [10] is modified to estimate disturbance in any direction for each space robot and then compensate it in the controller. The block diagram of the controller combined with the second order observer is shown in the Fig. 4. Note that the inputs and outputs of the blocks in the Fig. 4 are vector contrary to Ref. [4].

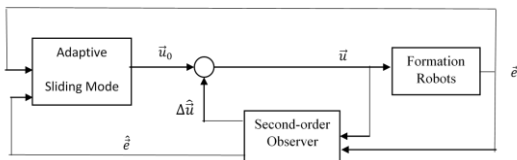


Fig. 4: block diagram of the controller combined with the second order observer

According to Eq. (14), to adapt the observer for the problem considered in this paper, the error dynamics can be written as follows:

$$\begin{aligned} \ddot{\vec{e}}_n(t) &= \ddot{\vec{q}}_n^d(t) - \ddot{\vec{q}}_n(t) = \\ &= \frac{1}{m_n}(-C(\omega)\dot{q}_n - N(\vec{q}, \omega, \vec{R}) + \vec{F}_n^c + \vec{F}_n^d) \end{aligned} \quad (24)$$

$n = 1, \dots, 4$

Without loss of generality, it is assumed that the masses of space robots are  $m_n = 1$  and  $\Delta\vec{\rho}_n = -\vec{F}_n^d$  as well as  $\vec{u}_n = \ddot{\vec{q}}_n^d - \vec{F}_n^c$ . To rewritten the error dynamics in state space form, the following variables are considered:

$$\begin{cases} \vec{x}_1 = \vec{e}_n \\ \vec{x}_2 = \dot{\vec{e}}_n \\ \Delta\vec{u} = \Delta\vec{\rho}_n \\ \vec{u} = \vec{u}_n \end{cases} \quad (25)$$

So, we have:

$$\begin{cases} \dot{\vec{x}}_1 = \vec{x}_2 \\ \dot{\vec{x}}_2 = \Delta\vec{u} + \vec{u} \end{cases} \quad (26)$$

The second-order observer is considered as follows:

$$\begin{cases} \dot{\vec{\chi}}_{1n} = \vec{\chi}_{1n} \\ \dot{\vec{\chi}}_{1n} = \vec{\chi}_{2n} - \gamma_3 |\vec{\chi}_{1n} - \vec{x}_{1n}|^{2/3} \times \\ \quad \text{sign}(\vec{\chi}_{1n} - \vec{x}_{1n}) \\ \dot{\vec{\chi}}_{2n} = \vec{u}_n + \Delta\vec{u}_n \\ \Delta\vec{u}_n = -\gamma_2 |\vec{\chi}_{2n} - \vec{x}_{1n}|^{1/2} \times \\ \quad \text{sign}(\vec{\chi}_{2n} - \vec{x}_{1n}) + \vec{\chi}_{3n} \\ \dot{\vec{\chi}}_{3n} = -\gamma_1 \times \text{sign}(\vec{\chi}_{3n} - \Delta\vec{u}_n) \end{cases} \quad (27)$$

In the Eq. (27),  $\vec{\chi}_1, \vec{\chi}_2, \Delta\vec{u}$ , and  $\vec{\chi}_3$  are the observed values of  $\vec{x}_1, \vec{x}_2, \Delta\vec{u}$ , and  $\vec{u}$ , respectively. Also,  $\gamma_1, \gamma_2$ , and  $\gamma_3$  are constants to be chosen.

Note that the above observer should be employed for any of the space robots in each direction. For this reason, the relations in Eq. (27) are vector.

### 4. Simulation and Results

In order to simulate the problem, the system dynamics is represented in the state space form for  $n = 1, 2, 3, 4$ :

$$\begin{Bmatrix} \dot{\vec{q}}_{1n} \\ \dot{\vec{q}}_{2n} \end{Bmatrix} = \begin{Bmatrix} \vec{q}_{2n} \\ \vec{F}_n^c + \vec{F}_n^d - C\dot{q}_{2n} - N \end{Bmatrix} \quad (28)$$

Where  $\vec{F}_n^d = -\mu_n \vec{q}_n$ ,  $\mu_1 = 0.56$ ,  $\mu_2 = 0.48$ ,  $\mu_3 = 0.32$ , and  $\mu_4 = 0.65$ . The simulation parameters have been reported in Table 1.

parameters	value
$K_D$	2
$\lambda$	5
$\epsilon_0$	0.001
$\kappa$	10
$\tau$	0.01
$\eta$	10

The masses of robots are equal to  $m_1 = m_2 = m_3 = m_4 = m_{real} = 200 \text{ kg}$  in the dynamic model. To examine the robustness of the presented method in the presence of parametric uncertainties, it is assumed 20% mass uncertainty in the controller. Thus, we have  $m_1 = m_2 = m_3 = m_4 = 1.2m_{real} = 240 \text{ kg}$ .

#### 4.1. Results and discussion

In the following, the actual and desired paths are drawn in a graph for each robot to compare.

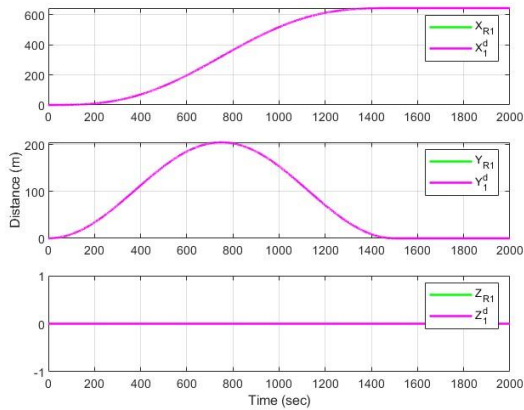


Fig. 5: The actual and desired paths for space robot 1 along x direction, y direction, and z direction

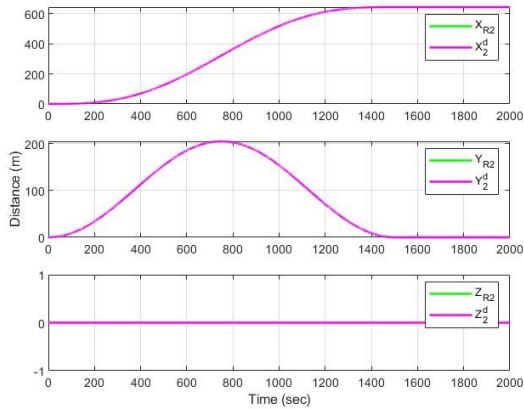


Fig. 6: The actual and desired paths for space robot 2 along x direction, y direction, and z direction

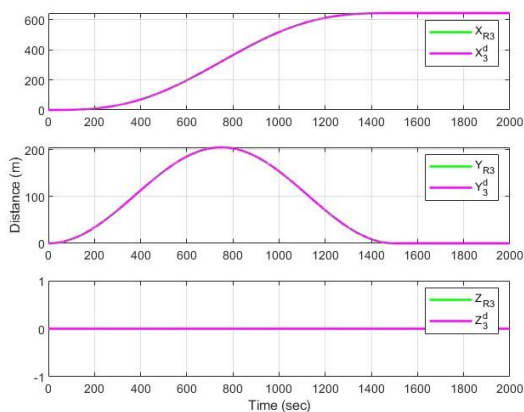


Fig. 7: The actual and desired paths for space robot 3 along x direction, y direction, and z direction

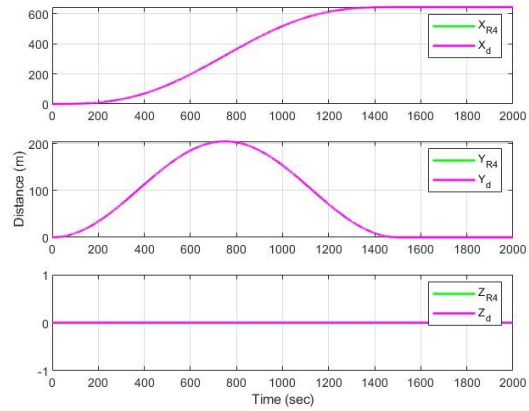


Fig. 8: The actual and desired paths for space robot 4 along x direction, y direction, and z direction

The tracking error of desired path for each of the space robots along x, y, and z direction is drawn in Figs. 9-12.

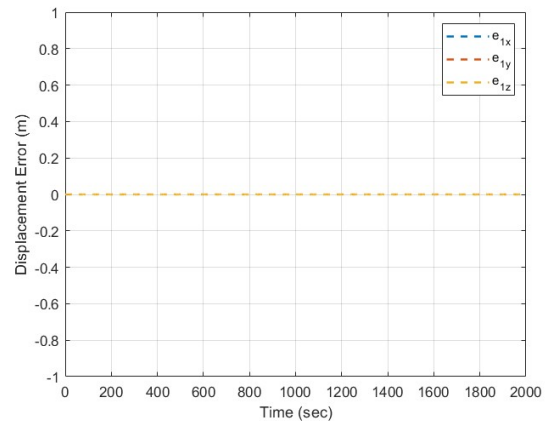


Fig. 9: The tracking error for space robot 1

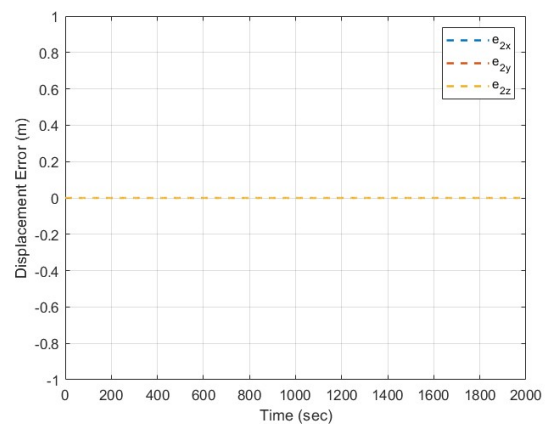


Fig. 10: The tracking error for space robot 2

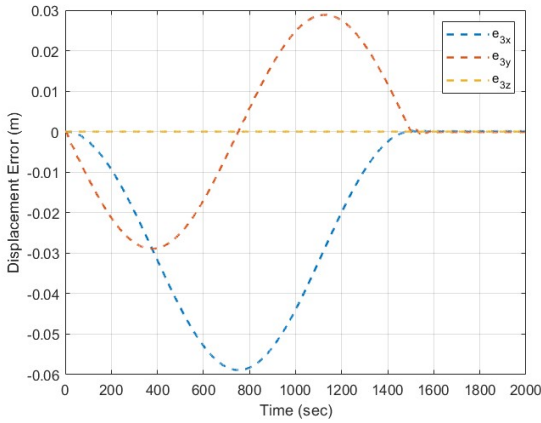


Fig. 11: The tracking error for space robot 3

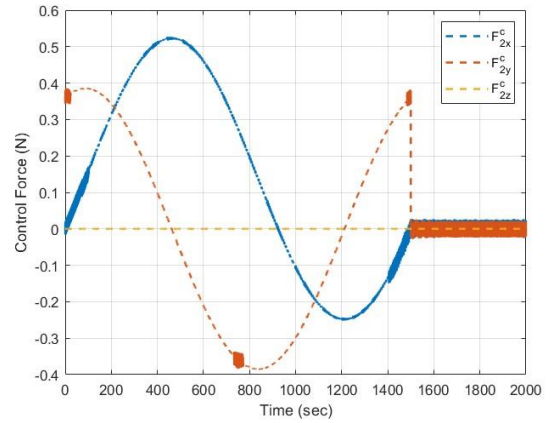


Fig. 14: The control force of the space robot 2

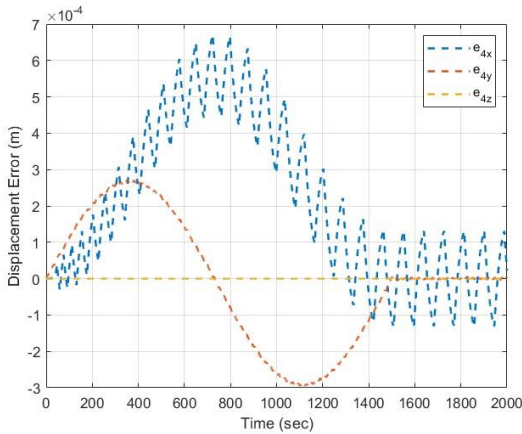


Fig. 12: The tracking error for space robot 4

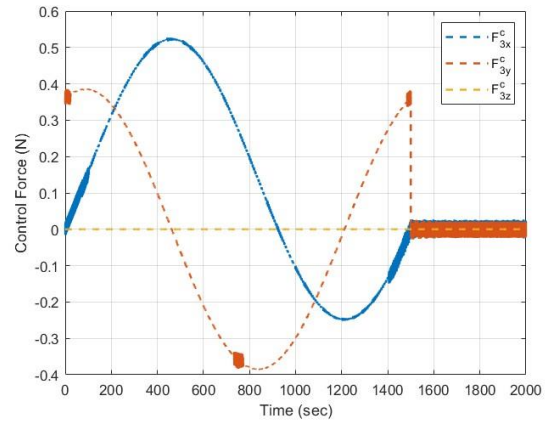


Fig. 15: The control force of the space robot 3

The control forces of the space robots are shown in Figs. 13-16.

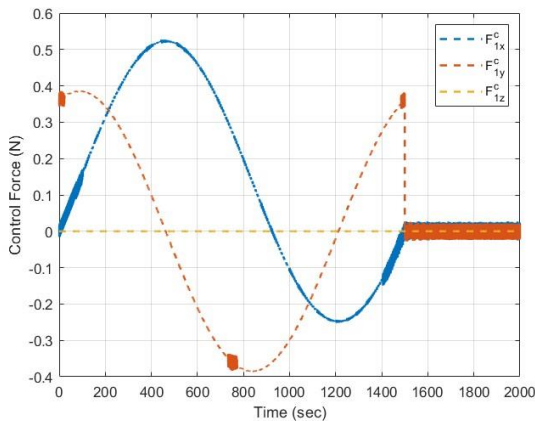


Fig. 13: The control force of the space robot 1

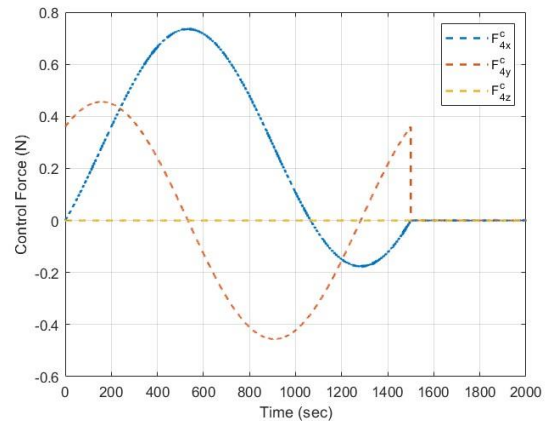


Fig. 16: The control force of the space robot 4

As it can be seen from the Figs. 9-12, the controller truly realizes the control objective. The trajectory tracking error of the fourth robot is on the order of  $10^{-4}$  meter i. e., 0.1 millimeter as well as for the third robot it is on the order of centimeter. Also, as it is clear from the Figs. 5-8, all of the space robots have tracked the desired path well.

### 5. Concluding Remarks and Future Work

This paper presents the formation control of space robots in order to on-orbit assembly of large solar sails.

The full nonlinear dynamic model of the formation consisting of four on-orbit space robots is derived using the leader-follower approach. Then, an adaptive sliding mode controller is developed for the derived model. Moreover, a second-order observer is embedded in the system to overcome the uncertainties including the unmolded dynamics, parameter uncertainties, and external disturbances. Eventually, simulation results indicate that the space robots track the desired trajectory with a good accuracy to deploy the solar sail. Future works will focus on considering the attitude control of the solar sail during the assembly of the sail and also the flexibility of the supporting booms of the sail.

## 6. References

- [1] J. Baculi and M. A. Ayoubi, "Fuzzy attitude control of solar sail via linear matrix inequalities," *Acta Astronautica*, vol. 138, pp. 233–241, Sep. 2017.
- [2] B. Wie and D. Murphy, "Solar-sail attitude control design for a flight validation mission," *Journal of Spacecraft and Rockets*, vol. 44, no. 4, pp. 809–821, Jul 2007.
- [3] Y. Tsuda and et al., "Flight status of IKAROS deep space solar sail demonstrator," *Acta Astronautica*, vol. 69, pp. 833–840, Nov. 2011.
- [4] Q. Hu, and et al., "Formation control of multi-robots for on-orbit assembly of large solar sails," *Acta Astronautica*, vol. 123, pp. 446–454, Jun. 2016.
- [5] B. Fu, and F. O. Eke., "Attitude control methodology for large solar sails," *Journal of Guidance, Control, and Dynamics*, vol. 38, no. 4, pp. 662–670, Apr. 2015.
- [6] D. A. Spencer, and et al., "Solar sailing technology challenges," *Aerospace Science and Technology*, vol. 93, pp. 105276, Oct. 2019.
- [7] B. Woo, and et al., "Deployment experiment for ultralarge solar sail system (ultrasail)," *Journal of Spacecraft and Rockets*, vol. 48, no. 5, pp. 874-880, Sep. 2011.
- [8] X. Bo, and Y. Gao, "'Sliding mode control of space robot formation flying," in *2009 IEEE International Conference on Autonomous Robots and Agents*, Wellington, New Zealand, 2009, pp. 561–565.
- [9] M. S. De Queiroz, and et al., "Adaptive nonlinear control of multiple spacecraft formation flying," *Journal of Guidance, Control, and Dynamics*, vol. 23, no. 3, pp. 385-390, May. 2000.
- [10] L. Fridman, and A. Levant, "Higher order sliding modes," *Sliding mode control in engineering*, vol. 11, pp. 53-102, Jan. 2002.